Chloride Penetration into Concrete after Uniaxial Compression

Xiaomei Wan*1, Folker H. Wittmann[2], Tiejun Zhao[3], Fuxiang Jiang[4]

[1,3,4]School of Civil Engineering, Qingdao Technological University, 11, Fushun Road, 266033 Qingdao, China
[2]Aedificat Institute Freiburg, 80, Schlierbergstr., D-79100 Freiburg, Germany
*1wanxiaomeiqj@126.com; [2]wittmann@aedificat.de; [3]ztjgp@263.net; [4]jfxwyt@163.com

***Abstract*- A non-destructive method of evaluation of volumetric strain due to microcracking was used to characterise microcracking in concrete prisms under uniaxial compression. Chloride profiles were also measured after the same concretes were exposed to chloride environment. The relationship among microcracking, stress level and chloride penetration of concrete was analysed based on the experimental results. Under compressive load the apparent chloride diffusion coefficient decreases until about one third of the ultimate load. Further increase of compressive load increases the chloride diffusion coefficient again. There is a close link between microcracking and stress level. The index of volumetric strain due to microcracking can be used to indicate the microcracking and study chloride transport into concrete under the influence of microcracking.**

Keywords- Concrete; Uniaxial Compression; Microcrack; Chloride; Volumetric Strain

I. INTRODUCTION

Mass transport properties of concrete can be changed by crack evolving under mechanical load. There are some initial cracks in concrete for the reasons of shrinkage, bleeding, thermal gradient, freezing, alkali aggregate reaction, etc. The initial cracks may propagate and more microcracks may be induced under external mechanical and environmental load. More cracks can form potential flow channels for aggressive ions such as chloride penetrating into concrete. The effect of cracks on the transport properties of concrete has been reported recently [1-6]. Most reports indicated that microcracks are significant to the permeability or capillary absorption of concrete.

Samaha and Hover [7] reported that microcracking in concrete at compressive stress levels below 75% of the ultimate stress did not affect the transport properties of concrete. The microcracks were quantified in terms of crack length by examining a concrete slice cut from a cylinder after the compression test. Then transport properties were measured by the rapid chloride permeability test in accordance with ASTM C1202. Saito and Ishimori [8] found the chloride permeability of concrete that had been loaded to 90% of the compressive strength to be nearly equal to that of unloaded control specimens. Through comparison of specific crack area for concrete cylinders subjected to uniaxial compression tests, Loo [9] reported that the microcracks become unstable and begin to propagate rapidly at stress level between 70% and 90% of the compressive strength. Lim [10] loaded the concrete cylinders to the level of 30%～95% of compressive strength and quantified the microcracks by specific crack area similar with Loo. Then the rapid chloride permeability test was also carried out. Lim concluded the chloride permeability is governed by the critical stress. When the critical stress is exceeded in a concrete specimen, a comparatively large electrical charge passed was measured. Where the critical stress in a specimen is not exceeded, the increase in the charge passed is marginal in spite of the large increase in microcracks. Ultrasonic evaluation [11], digital image correlation [12, 13] and acoustic emission [14] were also utilized as nondestructive cracking characterizations in recent years.

Gérard and Marchand [15] assessed theoretically the effect of crack networks on the steady-state diffusion properties of concrete using an analytical approach. Results of the theoretical analysis were then compared to experimental data. The results got from theoretical model indicated that the influence of cracks on diffusion properties is enhanced with increase of D1/D0, where D1 is the diffusion coefficient of ion in free solution and D0 is the diffusion coefficient of ion in uncracked homogeneous matrix. Other researchers [16] found that the crack length obeys log-normal distribution, and the crack orientation and connectivity are correlated strongly with crack density. The volumetric density is identified as a consistent parameter to describe the impact of crack network on altered transport properties.

Diane et al [17] discussed and amended experimentally the capillary flow theory in discrete cracks in cementitious materials. In the amendments, stick－slip behavior of the meniscus, frictional dissipation at the meniscus wall boundary and slip between the fluid and solid wall were considered. Recently the effects of crack geometry (i.e., width, tortuosity, and surface roughness) on chloride penetration [3] or water permeability [18] were also investigated and reported.

Although the link of microcracks and transport has been recognized widely, some conflicting results can be found through references review. In this paper a non-destructive method was used to characterise microcracking in concrete prisms during uniaxial compression. For revealing the effect of microcracking on the transport properties of concrete, the relationship among microcracking, stress level and chloride penetration of concrete was also analysed based on the experimental results.

II. MICROCRACK ASSESSMENT

Measurement of microcrack can be classified into two types. Visual observation (direct method) with some assistant technology, which involves observation of surface crack or the cracks on the sawed slice from specimen, and the measurement of deformation, Poisson's ratio, elastic modulus which can be used to evaluate the crack development indirectly. Besides surface strain, the latter also includes the measurement of ultrasonic pulse velocity, acoustic emission, measurement of cumulate energy consumption.

In direct method, slices usually need to be sawn from specimen after unloading and the transverse cracks can be observed. However, since sawing, colouring and grinding may produce new microcracks, much caution is needed during the whole operation. Furthermore, the observed cracks after unloading differ significantly from the one under sustained load.

The microcracks are characterised in terms of net change of volumetric strain compared with the one under the ideal linear elastic state during the test. The formula was derived on the assumption that the change in volumetric strain of a prismatic concrete specimen under uniaxial compression is equal to the sum of the elastic change in volumetric strain and the expansion due to microcracking,

$$\varepsilon_v = \varepsilon_{ve} + \varepsilon_{vcr} \tag{1}$$

where ε_v is the total volumetric strain of concrete, ε_{ve} is the elastic change in volumetric strain and ε_{vcr} is the volumetric strain due to microcracking.

ε_{ve} can be calculated linearly as the following,

$$\varepsilon_{ve} = (2\nu_e - 1)\varepsilon_l \tag{2}$$

and ε_{vcr} can be calculated as

$$\varepsilon_{vcr} = \varepsilon_v - \varepsilon_{ve} = 2\varepsilon_t - \varepsilon_l - (2\nu_e - 1)\varepsilon_l = 2(\varepsilon_t - \nu_e \cdot \varepsilon_l) \tag{3}$$

where ε_l is the longitudinal strain of concrete, ε_t is the transversal strain of concrete, and ν_e is the elastic Poisson's ratio. Both ε_l and ε_t are absolutely strain value. Early research [19] indicates that at the elastic stage when strain and stress develop linearly, normally below the stress level of 30%~50%, Poisson's ratio varies in the range of 0.15 to 0.24. If the stress continues to increase, Poisson's ratio will become unstable in turn. For reducing the error from the nonlinear stage, ν_e is determined from the initial elastic stage and ν_e should be stable in this paper.

III. EXPERIMENTAL

A. *Preparation of Specimens*

Two concrete mixes (C1 and C2) were selected for these investigations by using ordinary Portland cement P.O 42.5 and Class Ⅱ fly ash as binding materials. Locally available river sand and crushed gravel with maximum size of 25 mm were used. A naphthalene-based superplasticizer was added to the concrete mixture for enough workability. The compositions of the two mixes of concrete are given in Table 1.

The prisms of 100×100×400 mm were cast for these experiments. The molds of all specimens were removed after 24 h of casting, and the young specimens were further stored in the saturated solution of calcium hydroxide with a temperature of (20±3) ℃ until the age of test.

TABLE 1 MIX COMPOSITION OF THE SPECIMENS

	Cement (kg/m^3)	**Fly ash (kg/m^3)**	**Sand (kg/m^3)**	**Gravel (kg/m^3)**	**Water (kg/m^3)**	**W/B**	**f cu at 28 days (MPa)**
C1	306	77	754	1131	180	0.47	43.5
C2	383	0	754	1131	180		46.0

B. *Compressive Loading and Chloride Exposure*

At the age of 28 days, the compressive strengths of prisms were tested which are shown in Table 1 Then the specimens were compressed uniaxially to a preselected stress levels (0, 20%, 30%, 50% and 80%) of the ultimate strength and lasted for 5 minutes, then the loads were removed at a rate which was the same as that of the loading phase. Four strain gauges were glued on the lateral mould surface of each specimen, one in axial and one in transverse direction on each surface. The gauges were positioned at the mid-height of the specimen. During the period of loading and unloading, the strains were measured and thus the volumetric strain due to microcracking could be evaluated according to Eq. (3).

The gauges were removed from the specimens after unloading and the surfaces were cleaned completely. Then the specimens were saturated and immersed in the sodium chloride solution with mass concentrate of 5%. The surfaces where the strain had been measured were the exposed surface to chloride while the other surfaces were sealed with epoxy resin. After 1 month or 2 months, the specimens were taken out and milled by layers of 1 to 2 mm from the exposed surface. The chloride content of the powder obtained was determined by the silver nitrate titration method [20].

IV. STRAIN RESULTS

Plot of stress-strain variations during the load application and unload is shown in Fig. 1. The variation of transversal strain was analyzed besides longitudinal strain. Loo [9] and Lim [10] had researched experimentally the critical stress level at which concrete volumetric strain became a minimum and then expanded. Loo reported that the critical stress level was found to be between 0.83 and 0.91. In Lim's study, the critical stress was found to be exceeded in part specimens that have been loaded between 0.8 f_c and 0.95 f_c where the critical stress did not exceed 0.8 f_c and 0.85 f_c. However, the critical stress had not been found in the study where the maximum stress level was 0.8.

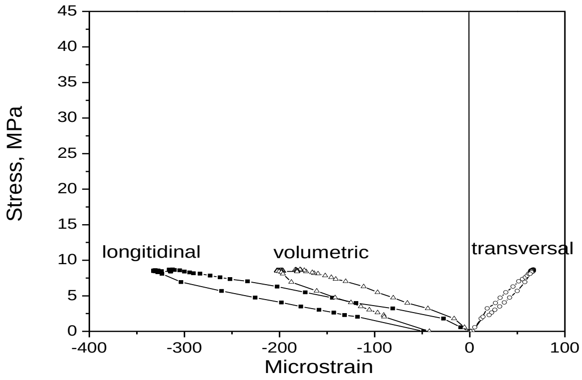

(a) C1-20%

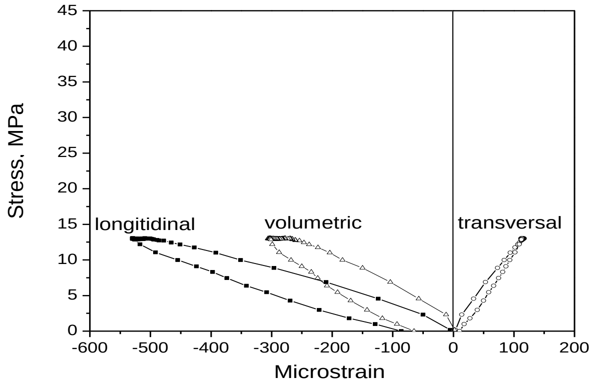

(b) C1-30%

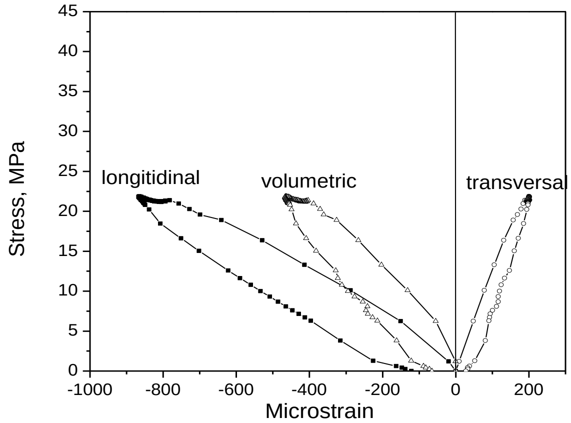

(c) C1-50%

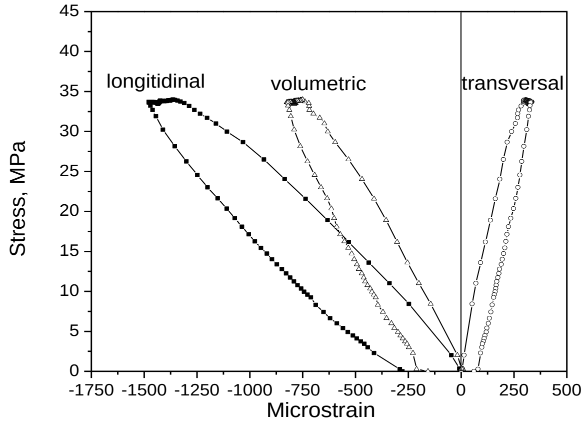

(d) C1-80%

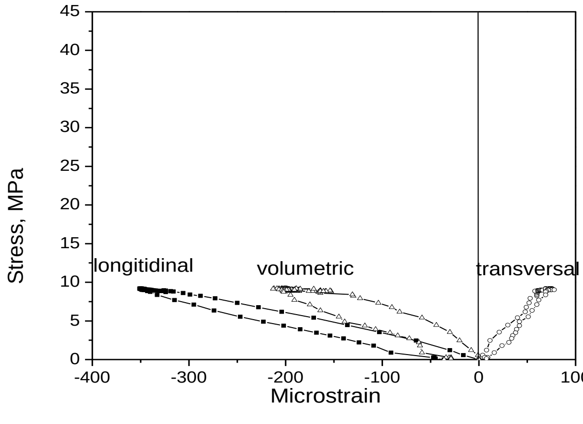

(e) C2-20%

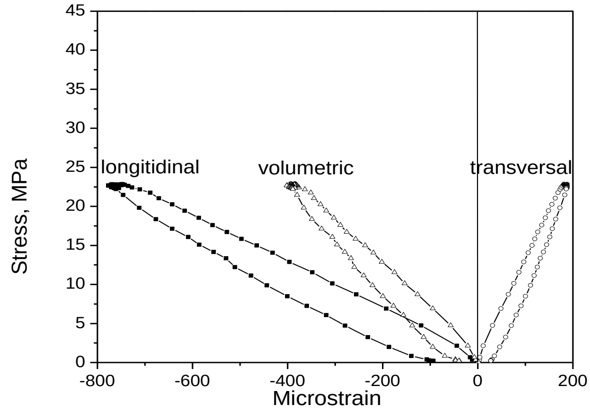

(f) C2-50%

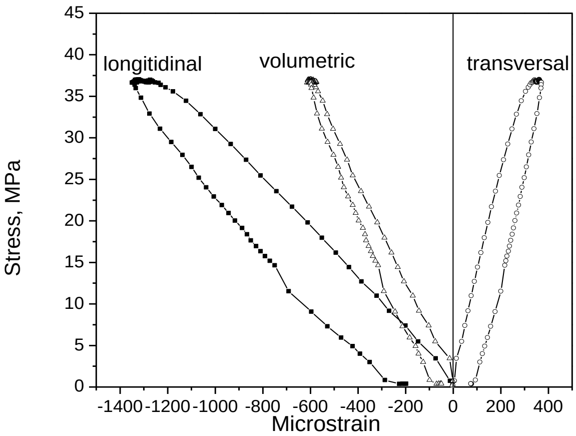

(g) C2-80%

Fig. 1 Stress and strain graphs of concrete

The volumetric strain due to microcracking (ε_{vcr}) calculated through Eq. (3) is given in Fig. 2. Initially with stress level less than 0.4, the volumetric strain due to microcracking develops little. It means that there is no significant development of microcrack at a low stress level and nearly all the ε_{vcr} resume zero after unloading (Fig. 2 except for (d) and (g)). When stress exceeds a certain level, the ε_{vcr} begins to increase greatly. In a general view of results, the certain stress level is in a wide range of 0.3 to 0.7. For the two mix proportions in the study, the stress level of C1where the ε_{vcr} begins to increase is from 0.5 to 0.7, while that of C2 is from 0.3 to 0.5. It seems that admixture of fly ash has the effect of elevating the critical stress level.

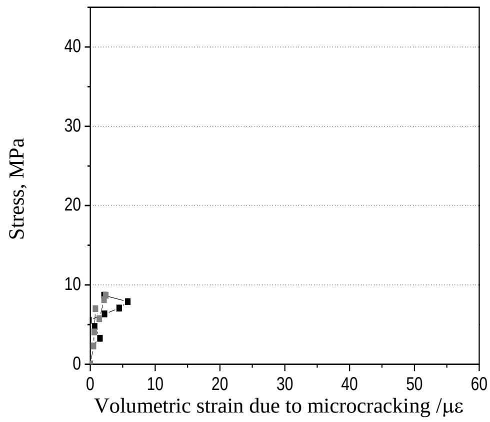

(a) C1-20%

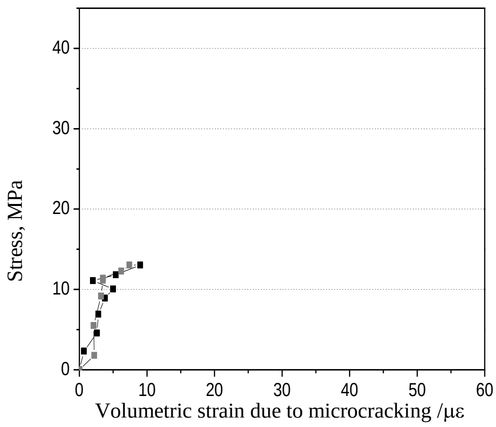

(b) C1-30%

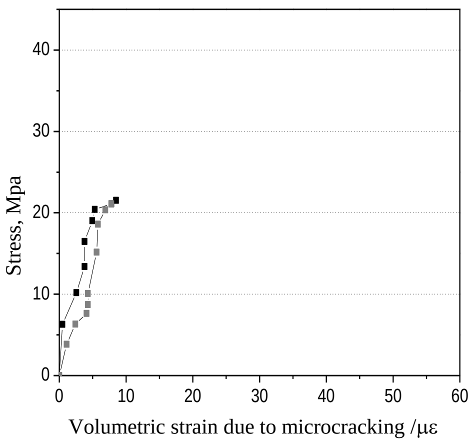

(c) C1-50%

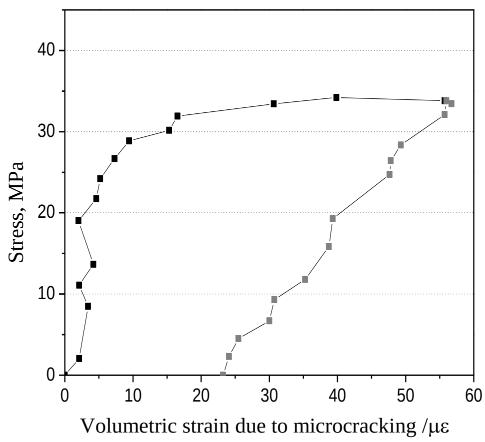

(d) C1-80%

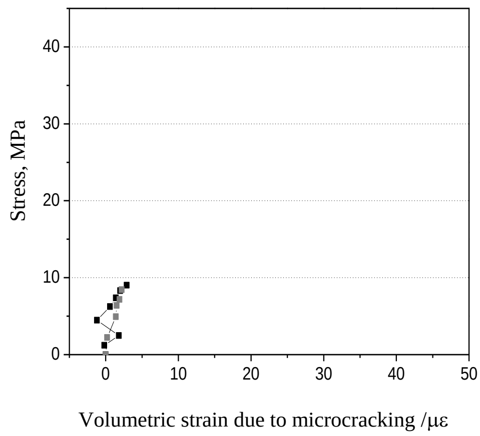

(e) C2-20%

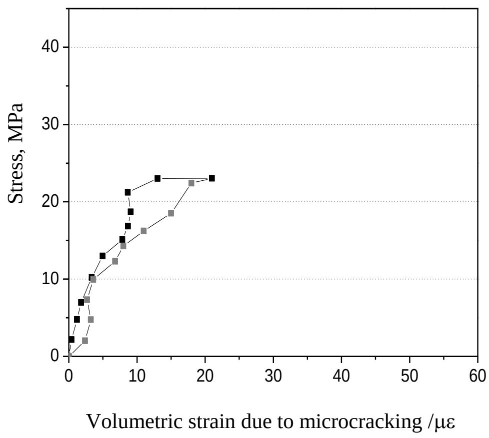

(f) C2-50%

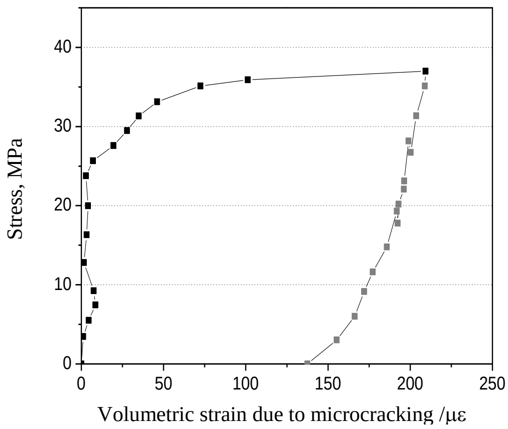

(g) C2-80%

Fig. 2 Volumetric strain due to microcracking of concrete

In the period of unloading, the ε_{vcr} decreases with the stress level. Because of microcrack developing, there is a certain residue ε_{vcr} when the load is removed completely. It can be found that there is a relationship between the residue ε_{vcr} and the ultimate stress level in Fig. 3. For C1, there is nearly no residue ε_{vcr} if loaded not beyond the stress level of 0.5, and there is a residue ε_{vcr} of 23.2 με if loaded to the stress level of 0.8. For C2, there is also no residue ε_{vcr} if loaded not beyond stress level of 0.5; however, there is a residue ε_{vcr} of 137.5 με if loaded to the stress level of 0.8. Obviously, the residue ε_{vcr} of specimens with fly ash admixture is less than the one of pure cement concrete.

Depending on the former results [21], it can be found that the residue damage in concrete is obvious when the load level is up to 0.7. Even when the load is removed, the influence of residue damage on the service performance should be treated seriously. Reference [10] concluded that some residue specific crack areas are observed when unloaded at the stress level of between 0.7 and 0.95, which implies only a partial closure of the microcracks. However, the critical stress level, at which significant ε_{vcr} is left subsequent to unloading, varies with the strength grade and mix proportion of concrete.

V. CHLORIDE CONTENT PROFILES

Chloride profiles in concrete which were measured after the specimens were immersed in solution of 5% sodium chloride for 1 or 2 months are given in Fig. 3. It can be found that the contents of penetrated chloride in C1 with fly ash are lower than C2. The pozzolanic reaction and spherical shape of fly ash particles decrease the penetration of chloride into concrete significantly. Under compressive load the chloride diffusion coefficient decreases until at the stress of 20%~30% of the ultimate load. However, further compressive load increases the content of penetrated chloride into concrete again. It may be assumed that the microstructure becomes denser initially and then microcracks develop through which chloride migration dominates.

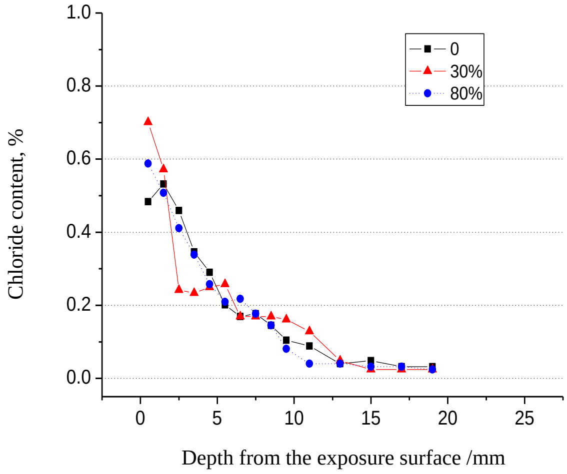

(a) C1 (1 month)

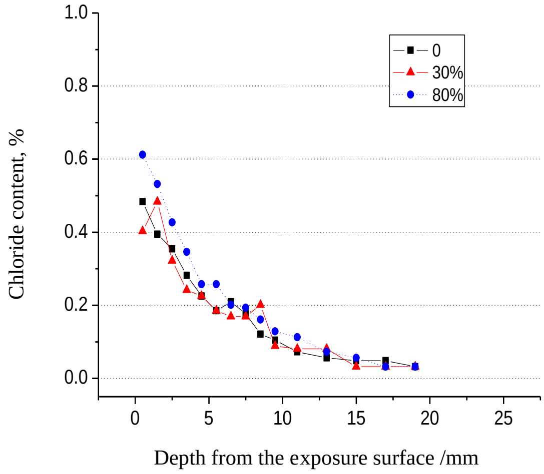

(b) C2 (1month)

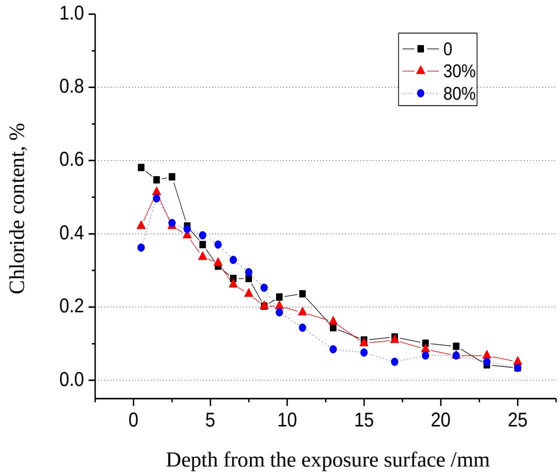

(c) C1 (2 months)

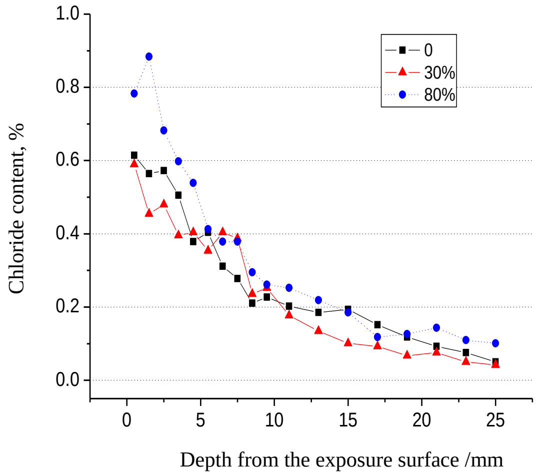

(d) C2 (2 months)

Fig. 3 Chloride profile in concrete

For the concretes exposed to salt solutions by immersion, Fick′s second law (Eq. (4)) was used to determine the chloride diffusion coefficient. According to $C(x, t)$, the chloride content profile in concrete with depths from exposure surface after a certain exposure duration t, the apparent chloride diffusion coefficient can be calculated by error function as given in Table 2, and the values in brackets represent the relative value of chloride diffusion coefficient compared with the one of unloaded concrete. Even though the concretes were cured in solution of calcium hydroxide and saturated in water before exposure to chloride, the penetration of chloride was influenced by capillary effect in a certain degree. Therefore, the apparent chloride diffusion coefficients in Table 2 are only a measure used to compare the different chloride transport performances in concrete.

$$C(x,t) = C_0 + (C_s - C_0)\cdot\left[1-\mathrm{erf}\,(\frac{x}{2\sqrt{Dt}})\right] \tag{4}$$

where, x is the depth in concrete from exposure surface, t is the exposure duration, C_0 is the value of chloride initial content, C_s is the value of chloride surface content, D is the apparent chloride diffusion coefficient, erf(z) is the error function, $\mathrm{erf}\,(z) = \frac{2}{\sqrt{\pi}}\int_0^z \exp(-z^2)\mathrm{d}z$.

TABLE 2 APPARENT CHLORIDE DIFFUSION COEFFICIENT OF MECHANICAL LOADED CONCRETE

Exposure duration	**Specimens**	**Stress level**	**Apparent chloride diffusion coefficient, 10^{-6}mm^2/s**

1 month	C1	0	7.82 （1）
		0.3	7.45 （0.95）
		0.8	7.76 （0.99）
	C2	0	10.09 （1）
		0.3	9.68 （0.96）
		0.8	10.62 （1.05）
2 months	C1	0	5.95 （1）
		0.2	5.35 （0.90）
		0.3	5.65 （0.95）
		0.5	6.07 （1.02）
		0.8	6.42 （1.08）
	C2	0	7.32 （1）
		0.2	7.18 （0.98）
		0.3	7.24 （0.99）
		0.5	7.62 （1.04）
		0.8	8.58 （1.17）

Similar to the trend of measured chloride content profile, under compressive load the apparent chloride diffusion coefficient first decreases up to a load level of approximately 30% of the ultimate load. If, however, the compressive load increases further, the apparent chloride diffusion coefficient increases with compressive load.

It can be found from the results of Table 2 that the apparent chloride diffusion coefficient of concrete of 2 months exposure is 17%~27% lower than the concrete of 1 month, which implies the regress with time effect of chloride diffusion coefficient of concrete in nature exposure.

VI. RELATIONSHIP BETWEEN STRESS, MICROCRACKS AND CHLORIDE PENETRATION

Depending on the experimental results, the residue volumetric strain due to microcracking and apparent chloride diffusion coefficient are plotted in Fig. 4. For the concrete compressed and then unloaded, the chloride diffusion coefficient decreases in the initial range of approximately 30% of the ultimate load. However, further compressive load increases the content of chloride penetration into concrete. It may be assumed that the microstructure becomes denser firstly and then microcracks develop through which chloride migration dominates that even exceeds the one without load. In the case of C2 with 2 months exposure, the apparent chloride diffusion coefficients of concrete loaded to stress level of 0.2 and 0.3 decrease to 90% and 95% of the ones of concrete without load respectively. When the stress level increases to 0.5, the apparent chloride diffusion coefficient increases again to the level of concrete without load, and when the stress level increases to 0.8, the apparent chloride diffusion coefficient increases to 1.08 times the one without load.

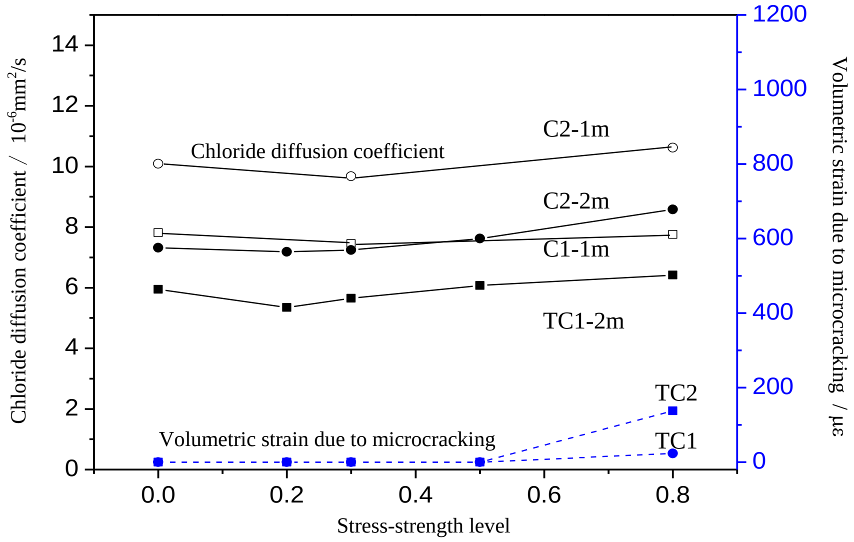

Fig. 4 Residue volumetric strain due to microcracking and chloride diffusion coefficient under different stress levels

As mentioned before, there is a close relationship between the evolvement of microcracks and the load level in the experimental research. For both concrete C1 and C2, there is nearly no residue volumetric strain due to microcracking when the load is not beyond the stress level of 0.5, and the apparent chloride diffusion coefficient is kept as near or lower than the one of concrete without load. However, when the stress level increases to 0.8, the residue volumetric strains due to microcracking of C1 and C2 attain to 23.2 με and 137.5 με, and the apparent chloride diffusion coefficients increase to 1.08 and 1.17 times the ones without load respectively. It implies that there is more evolvement of microcracks in C2 (without fly ash admixed) under uniaxial compression compared with C1 (with fly ash admixed). Therefore there is higher ε_{vcr} and more chloride penetration in C2 than in C1. It also shows that ε_{vcr} can be used to represent the evolvement of microcracks in concrete and analyze the effect of load-induced microcracks on the chloride transport in concrete. However, ε_{vcr} can not reflect the trend of concrete becoming denser under a relative low compressive stress level.

VII. CONCLUSIONS

The relationship among load level, microcracking and chloride permeability was investigated and conclusions are acquired as follows.

(1) For the concrete under uniaxial compressive load, the evolution and resume of microcracks relate to stress level closely. Initially with stress level less than 0.4, the residue volumetric strain due to microcracking develops little. It means that there is no significant evolvement of microcrack at a low stress level and nearly all the volumetric strains due to microcracking resume zero after load removed. However, when stress exceeds a certain level, the specific crack areas begin to increase greatly.

(2) There is a relationship between the residue volumetric strain due to microcracking and the highest stress level of compressive load when load is removed. The residue volumetric strain due to microcracking of specimens with fly ash admixture is less than the one of pure cement concrete if the load is removed at the stress level of 0.8.

(3) Under compressive load the apparent chloride diffusion coefficient first decreases until the stress level up to approximately 30% of the ultimate load. However, further increase of the compressive load increases the chloride penetration into concrete again. But the residue volumetric strain due to microcracking can not reflect the trend of concrete becoming denser under a lower compressive stress level.

(4) The volumetric strain due to microcracking can be used to represent the evolvement of microcracks in concrete and analyze the effect of load-induced microcracks on the chloride transport in concrete.

ACKNOWLEDGEMENTS

Financial supports from National Basic Research Program of China (973 Program) (2009CB623203) and Natural Science Foundation of Shandong Province (ZR2011EEQ031) are gratefully acknowledged.

REFERENCES

[1] B. Gérard, H.W. Reinhardt, and D. Breysse, “Measured transport in cracked concrete,” in Penetration and Permeability of Concrete: Barriers to Organic and Contaminating Liquids, H. E. Reinhardt, Ed. Stuttgart, Germany: E&FN Spon, p. 265–324, 1997.

[2] S. J. Jaffer and C. M. Hansson, “Chloride-induced corrosion products of steel in cracked-concrete subjected to different loading conditions,” *Cem Concr Res*, vol. 39, pp. 116–125, 2009.

[3] H. Ye, N. Jin, X. Jin, and C. Fu, “Model of chloride penetration into cracked concrete subject to drying - wetting cycles,” *Constr Build Mater*, vol. 36, pp. 259–269, 2012.

[4] D. Gardner, A. Jefferson, and A. Hoffman., “Investigation of capillary flow in discrete cracks in cementitious materials,” *Cem Concr Res*, vol. 42, pp.972–981, 2012.

[5] M. A. Glinicki and A. Litorowicz, “Crack system evaluation in concrete elements at mesoscale,” *Bulletin of the Polish Academy of Sciences, Tech Sci*, vol. 54, pp. 371–379, 2006.

[6] X. Wan, F. H. Wittmann, and T. Zhao, “Influence of mechanical load on service life of reinforced concrete structures under dominant influence of carbonation,” *Restor Build Monum*, vol. 17, pp. 103–110, 2011.

[7] H. R. Samaha and K. C. Hover, “Influence of microcracking on the mass transport properties of concrete,” *ACI Mater J*, vol. 89, pp. 416–424, 1992.

[8] M. Saito and H. Ishimori, “Chloride permeability of concrete under static and repeated compressive loadings,” *Cem Concr Res*, vol. 25, pp. 803–808, 1995.

[9] Y. H. Loo, “A new method for microcrack evaluation in concrete under compression,” *Mater Struct*, vol. 25, pp. 573–578, 1992.

[10] C. C. Lim, N. Gowripalan, and V. Sirivivatnanon, “Micro cracking and chloride permeability of concrete under uniaxial compression,” *Cem Concr Compos*, vol. 22, pp. 353–360, 2000.

[11] P. Antonaci, C. L. E. Bruno, P. G. Bocca, M. Scalerandi, and A. S. Gliozzi, “Nonlinear ultrasonic evaluation of load effects on discontinuities in concrete,” *Cem Concr Res*, vol. 40, pp. 340–346, 2010.

[12] S. Rouchier, H. Janssen, C. Rode, M. Woloszyn, G. Foray, and Roux J, “Characterization of fracture patterns and hygric properties for moisture flow modelling in cracked concrete,” *Constr Build Mater*, vol. 34, pp. 54–62, 2012.

[13] T. Mauroux, F. Benboudjema, P. Turcry, A. Ait-Mokhtar, and O. Deves, “Study of cracking due to drying in coating mortars by digital image correlation,” *Cem Concr Res*, vol. 42, pp. 10141023, 2012.

[14] H. Elaqra, N. Godin, G. Peix, M. R'Mili, and G. Fantozzia, “Damage evolution analysis in mortar, during compressive loading using acoustic emission and X-ray tomography: effects of the sand/cement ratio,” *Cem Concr Res*, vol. 37, pp. 703–713, 2007.

[15] B. Gérard and J. Marchand, “Influence of cracking on the diffusion propertied of cement-based materials, part 1: influence of continuous cracks on the steady-state regime,” *Cem Concr Res*, vol. 30, pp. 37–43, 2000.

[16] C. Zhou, K. Li, and X. Pang, “Geometry of crack network and its impact on transport properties of concrete,” *Cem Concr Res*, vol. 42, pp. 1261–1272, 2012.

[17] G. Diane, J. Anthony, and H. Andrea, “Investigation of capillary flow in discrete cracks in cementitious materials,” *Cem Concr Res*, vol. 42, pp. 972–981, 2012.

[18] A. Akhavan, S. Shafaatian, and F. Rajabipour, “Quantifying the effects of crack width, tortuosity, and roughness on water permeability of cracked mortars,” *Cem Concr Res*, vol. 42, pp. 313–320, 2012.

[19] X. Wan, “Deterioration mechanisms of reinforced concrete structures under combined mechanical and environmental action,” D. Eng. thesis, Xi’an University of Architecture & Technology, Xi’an, China, 2011. (in Chinese)

[20] JTJ 270-98 Testing Code of Concrete for Port and Waterwog Engineering; 1998. (in Chinese)

[21] X. Wan, T. Zhao, F. Jiang, and Q. Su, “Experimental research on carbonation performance of mechanical loaded concrete,” in Proceedings of the Fifth Symposium on Strait Crossings, K. Senneset, K. Flaate, H. Ostlid, Ed. Trondheim, Norway: Norwegian University of Science and Technology, pp. 525–530, 2009.

Xiaomei Wan, was born in Nanning, China in Dec. 1974. She first studies civil engineering at Qingdao Technological University and obtained the bachelor degree in 1997 and the master degree in 2002. She began to study the deterioration mechanism of reinforced concrete structures under combined mechanical and environmental action during her doctoral thesis work at Xi’an University of Architecture & Technology and obtained her doctor degree in 2011.

At present she is an associate professor of School of Civil Engineering at Qingdao Technological University, China. Her main work involves durability research of concrete structures and teaching the course of civil engineering materials.

Dr. Wan, Member of Technical Committee TC-TDC of RILEM.